

# Transient Behavior of Associating Copolymers in a Shear Flow

Rolf Klucker,<sup>†</sup> Françoise Candau,<sup>‡</sup> and François Schosseler<sup>\*,†</sup>

Laboratoire d'Ultrasons et de Dynamique des Fluides Complexes, URA 851, Université Louis Pasteur, 4 rue Blaise Pascal, 67070 Strasbourg Cedex, France, and Institut Charles Sadron, 6 rue Boussingault, 67083 Strasbourg Cedex, France

Received January 26, 1995; Revised Manuscript Received April 24, 1995<sup>\*</sup>

**ABSTRACT:** The transient response of associative copolymer solutions during step shear rate experiments has been characterized. Upon cessation of flow, the stress relaxation modulus is found to decrease faster as the shear rate increases. Upon start up of the flow, beyond a critical value of the shear rate, one or several stress overshoots are observed, depending on the shear rate value. One of them corresponds to the stress overshoot characteristic of entangled polymer systems while the other ones are specific to the presence of hydrophobic units. The critical shear rate and the accumulated strain position that characterize the appearance of the overshoots can be most easily explained if the solution is viewed as a loosely connected transient network. Finally, aging phenomena are also described and are tentatively ascribed to a trend to phase separation.

## 1. Introduction

Associative thickeners are of high interest in chemical industries. Water-soluble polymers modified with relatively small amounts of a hydrophobic comonomer have become the object of extensive research, because of their interesting rheological behavior.<sup>1-10</sup> Intermolecular interactions are increasing the zero-shear viscosity. However, these polymers show under shear a strong shear-thinning effect, since the physical interchain associations are disrupted. At high shear rate the viscosity of the homopolymer with the same molecular weight is recovered. This dissociation phenomenon is reversible, and under decreasing shear the interchain liaisons are reorganized. However, due to the time needed for new associations to be formed, hysteresis phenomena are often observed and then the initial zero-shear viscosity is recovered only after several hours of rest. While this behavior is well established and qualitatively understood, no attempts have been made to fully characterize the viscoelastic properties of these associative copolymers at various stages of the reorganization process. This was the primary aim of this work. However, in the course of the study, some new phenomena, as yet not reported in the literature, were observed. They are illustrated in Figure 1, which shows the establishment of the stress as a function of total accumulated strain,  $\gamma = \dot{\gamma}t$ , for different shear rates  $\dot{\gamma}$ , where  $t$  is the elapsed time since the beginning of the flow. As the shear rate increases, stress overshoots appear and eventually for the highest shear rates, multiple overshoots are observed which make the determination of a steady shear viscosity very difficult on the time scale of the experiment. Such behavior has not been reported before presumably because (a) data were mainly obtained on imposed stress devices while we performed our study with an imposed strain rheometer and (b) not enough rest time was allotted between two successive shear rate steps.

In this paper, we want to detail this behavior and to show that some information about the association of hydrophobic groups is contained in these overshoots, the height and position of which change with the time of rest between two experiments. We present also some

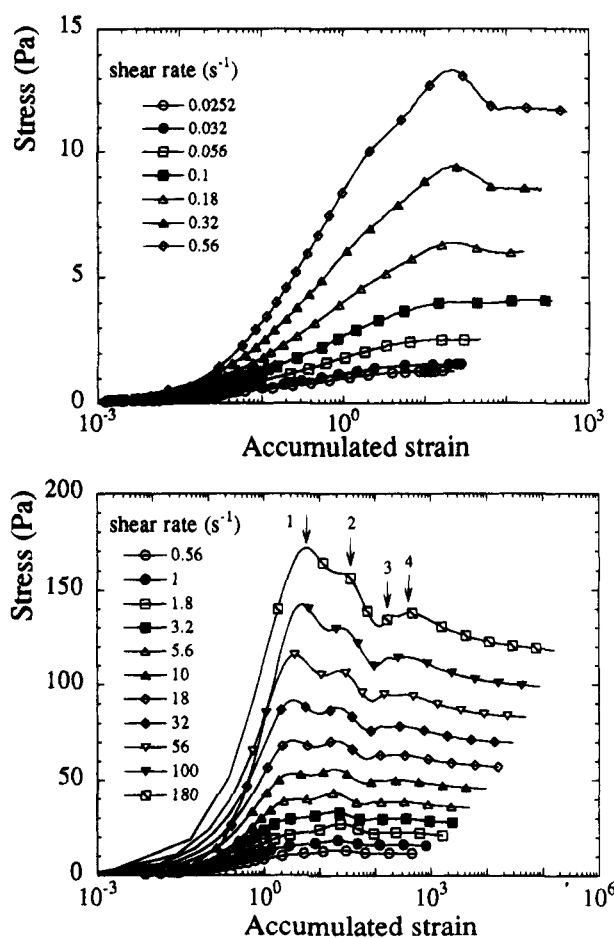


**Figure 1.** Evolution of the transient shear stress with accumulated strain for increasing shear rates (copolymer F with a 3% w/w concentration). Only one experimental point out of ten is pictured as a symbol. For the highest shear rates, the arrows indicate the overshoots indexed as in the text.

results on the time scale of stress relaxation and on the long-term evolution of the associating solutions.

## 2. Experimental Section

**2.1. Sample Synthesis.** The synthesis method has been described at length in preceding papers.<sup>6,7</sup> The associative copolymers are linear hydrophobically modified polyacrylamide (AM), with *N*-ethylphenylacrylamide as hydrophobic monomer.

<sup>†</sup> Université Louis Pasteur.

<sup>‡</sup> Institut Charles Sadron.

<sup>\*</sup> Abstract published in *Advance ACS Abstracts*, June 1, 1995.

Table 1. Characteristics of the Samples

polymer	surfactant concn (% w/w)	initial concn of hydrophobe (% mol)	reacn time	conv (%)	hydrophobe content (% mol)	mol wt ( $10^6$ g/mol)
A	2	1	7 h	85	1.08	2.8
F	3	0.75	15 min	11.3	1.17	3.8
H	3		15 min	3.61		3.8

They are obtained through a micellar radical copolymerization in water,<sup>5</sup> with sodium dodecyl sulfate (SDS) as surfactant and potassium persulfate ( $K_2S_2O_8$ ) as initiator. The use of a surfactant allows the solubilization of the hydrophobic monomer. The structure of the resulting copolymers consists of randomly distributed blocks of hydrophobic monomers in a mainly hydrophilic backbone. The average length of the hydrophobic blocks depends mainly on the initial composition of the feed comonomers and the hydrophobic monomer/surfactant concentration ratio. An additional parameter characterizing the resulting copolymers is the average compositional heterogeneity between chains synthesized at different reaction times. Assuming equal reactivity ratios of the monomers, the drift in average copolymer composition was attributed to micellar effects, resulting in a higher hydrophobe incorporation in the early stages of the polymerization.<sup>7,8</sup> Thus, copolymers at high conversion levels may contain homopolyacrylamide chains together with hydrophobe-rich chains. To reduce this effect, the reaction is stopped before full completion by adding a small amount of (methanol) hydroquinone and cooling the reaction bath. The polymer is then precipitated and repeatedly washed in methanol to remove surfactant and unreacted monomers. Finally, the polymer is dried and kept in tightly closed containers for further use. The weight-average molecular weight of the sample is obtained from static light scattering experiments performed on dilute solutions of the polymer in formamide. The content of hydrophobic units is measured by UV spectroscopy. Table 1 summarizes the characteristics of the samples.

**2.2. Rheological Measurements.** For the rheological experiments, a Rheometrics RFS II fluid spectrometer with a cone-plate geometry was used (radius = 2.5 cm; angle = 0.0397 rad; gap = 45  $\mu$ m). This machine was equipped with additional homemade gear that prevents evaporation of the sample during experiments with long duration times.

Different modi operandi can be thought of for the experiments. The first one (Figure 2a) involves successive shear rate steps with increasing (or decreasing) shear rates  $\dot{\gamma}$ , identical shear duration ( $\Delta t = 1000$  s), and constant short rest intervals ( $T = 30$  s) between the shear rate steps. This is the most common procedure used to investigate shear thinning and hysteresis effects. Only the steady shear viscosity can be obtained in these experiments. Therefore we preferred a second procedure which follows the same lines but with much larger rest times ( $T = 1000$  s) to allow a good measurement of both the steady shear viscosity and the stress relaxation in the samples. A third procedure (Figure 2b) consists of shear rate steps with identical duration and shear rate, separated by increasing rest intervals ( $30 < T < 5.6 \times 10^4$  s). The latter procedure is well suited to test the reorganization of the hydrophobic domains in the samples.

In our experiments, the applied shear rates ranged between  $2.52 \times 10^{-2}$  and  $560$  s<sup>-1</sup>. It has to be realized that, over such a wide range, the ability of the apparatus to realize ideal rectangular shear rate impulses is limited. However, no output signal is available to get the true instantaneous shear rate as a function of time. This is a problem when plots as a function of total accumulated strain are required. In particular, for high shear rates, the strain accumulated during the raising time can be quite comparable to the total strain accumulated at smaller shear rates. We solved that problem by performing step shear rates experiments on Newtonian oils with zero-shear viscosity in the same range as in our samples. By requiring a superposition of the increasing stress as a function of accumulated strain in these experiments, we were able to generate for each shear rate a correspondence between

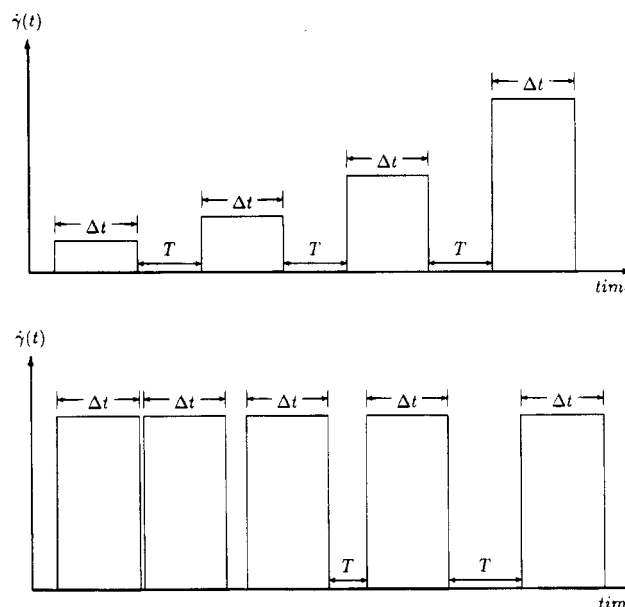


Figure 2. Sketch of the different shear histories used for the experiments.

elapsed time and true accumulated strain. This empirical relationship resisted any simple closed-form modeling and was applied numerically, when necessary, to our data. It can be noted that this relationship was found to be identical for three different Newtonian oils with viscosities 1.2, 12, and 60 Pa·s, showing that the main source for the deformation of the rectangular pulses is the inertia of the apparatus.

**2.3. Sample Preparation.** The preparation of a sample for an experiment is always the following. To a given amount of polymer is added the appropriate quantity of deionized water to obtain a 2 or 3% w/w concentration. The chains are allowed to hydrate and swell for 24 h. Then the sample is very gently stirred for another 24 h. After 2 more days of equilibration, the sample is ready for measurements, and this time is arbitrarily taken as the time origin for aging processes. This procedure allows one to obtain bubble-free solutions, whereas a direct stirring of the samples most often results in a foam unsuitable for these experiments. The samples are then gently loaded into the cone-plate tool and allowed to rest 0.5 h before testing. This allows reproducible zero-shear viscosity values. For experiments with a long duration (more than several hours), before and after each series of experiments, a dynamic frequency sweep with 3% applied strain is performed to check the aging of the sample.

### 3. Results

**3.1. Stress Relaxation.** The stress relaxation after a shear rate step should be followed by the procedure depicted in Figure 2a with a rest time  $T$  long enough to allow a complete relaxation of the stress. However, due to the long characteristic times involved, this procedure is too time-consuming and we had to keep a constant rest time  $T = 1000$  s for all the shear rates. At this point it is important to realize that an artifact introduced by the rheometer software can vitiate the data: before each rectangular impulse, the apparatus is performing an automatic calibration procedure that sets the initial recorded stress to zero. If the stress relaxation from the preceding step is not complete, this procedure introduces an offset between the new series of data stress and the actual stress in the sample. This effect appears clearly if the stress relaxation is followed for a long time in the last cycle since then the final equilibrium value of the stress is found to be negative. That artifact was corrected by propagating the offsets for the successive shear rate steps along the shear

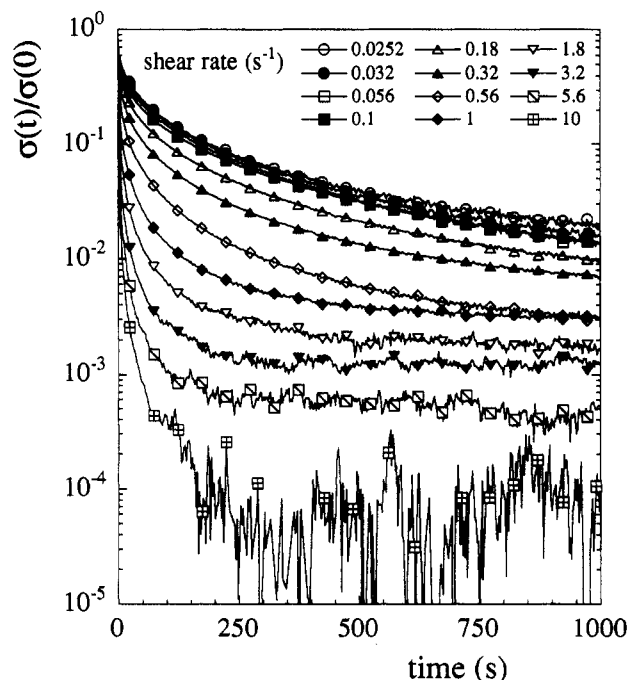


**Figure 3.** Shear stress decay after cessation of flow for different shear rates. Sample is copolymer F with a 3% w/w concentration. Curves are normalized by the initial shear stress as described in the text. Symbols correspond to every 20th experimental point.

history. Figure 3 shows the resulting relaxation curves normalized by the initial stress, corrected by the appropriate offset, at the beginning of each relaxation process. In this figure, the initial decay of the stress appears clearly steeper and steeper as the shear rate increases. Also the fast relaxation modes are responsible for an increasing fraction of the total stress relaxation. The behavior at longer times is less clear. While for the smallest shear rates ( $\dot{\gamma} \leq 1 \text{ s}^{-1}$ ), the long-time decay of the stress can be reasonably approximated by a single exponential, with a characteristic time about 890 s, independent of shear rate, the relaxation curves for shear rates above  $1 \text{ s}^{-1}$  seem to level off. However, this effect could result from an incorrect estimate of the offsets and has to be checked in new experiments.

**3.2. Stress Overshoots.** As depicted in Figure 1, characteristic multiple stress overshoots occur during the establishment of the stress when the shear rate is high enough. In this case four of them can be clearly distinguished and are indexed as indicated in Figure 1. The strain positions  $\gamma_{\max,i}$  of the first two are reported in Figure 4 as a function of the shear rate. As described in the Experimental Section, the strain is calculated here by an empirically determined relationship between the elapsed time and the accumulated strain. The shear history used to obtain the data in Figure 4 is the one depicted in Figure 2a with a rest time  $T = 1000 \text{ s}$  between two successive shear rate steps.

The two intermediate overshoots located at  $\gamma_{\max,2} \approx 20$  and  $\gamma_{\max,3} \approx 100$  appear as soon as  $\dot{\gamma} \geq 0.1 \text{ s}^{-1}$ , while the first one ( $\gamma_{\max,1} \approx 3$ ) and the last one ( $\gamma_{\max,4} \approx 300$ ) show up only for shear rates larger than, respectively, 1 and  $10 \text{ s}^{-1}$ . In fact, it is not clear if the distinction between the third and the fourth overshoots does not arise merely from a splitting of one bump in the stress. Therefore in the following, we do not discuss in detail their behavior and focus mainly on the first two overshoots. As a general trend, the positions of these overshoots seem practically insensitive to the shear rate

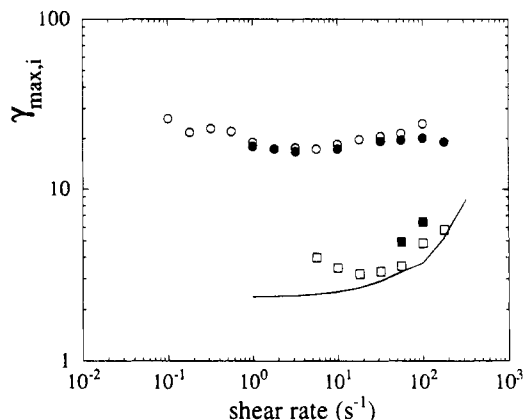


**Figure 4.** Evolution with shear rate of the strain position of the first (squares) and second (circles) overshoots. Sample is copolymer F with a 2% (closed symbols) or 3% (open symbols) w/w concentration. The continuous line shows for comparison the corresponding behavior of the homopolymer H with the same average molecular weight as copolymer F in a 3% w/w solution (see Table 1).

values when  $\dot{\gamma} < 10 \text{ s}^{-1}$  and increase weakly by a factor of the order of 2 when the shear rate is increased by a factor of 20, from 10 to  $200 \text{ s}^{-1}$ . Larger  $\dot{\gamma}$  values could not be measured due to the limitations of our torque transducer or the spilling of the sample out of the tool under centrifugal forces.

The same features are observed for a 2% solution of the same copolymer (Figure 4). The presence of one overshoot is also visible if the same experiment is carried on a 3% solution of an unmodified polyacrylamide (sample H) with the same molecular weight as copolymer F. The position of this overshoot (shown as a continuous line in Figure 4) is comparable with that of the first overshoot in the copolymer curves. As pointed out by a referee, the influence of chain length polydispersity could be questioned while comparing the behavior of samples H and F. However, these two samples were synthesized under the same conditions (except that no hydrophobic units were present in the case of the homopolymer) and therefore should have comparable molecular weight distributions. Moreover, the position of this overshoot does not depend on the chain length in the Doi-Edwards model as long as all the chains remain entangled. On the other hand, the critical shear rate for the appearance of the first overshoot should be markedly sensitive to the chain length distribution (see Discussion).

As emphasized in the Introduction, the rheological properties of associative thickeners often exhibit marked hysteresis effects. The same remark applies also to their transient response to a shear rate step. This is best exemplified if the second testing mode (Figure 2b) is applied to the sample. Figure 5 shows a detailed view of the stress curves recorded for constant shear rate steps ( $\dot{\gamma} = 56 \text{ s}^{-1}$ ), separated with increasing rest time intervals. A clear difference is observed between the behavior of the first overshoot, which is insensitive to the time lag between two steps, and the second one, which shows a definite dependence of its position (Figure 6a) and amplitude (Figure 6b) on the rest time allocated to the sample. Note that, for the first overshoot, we assess the different behavior in the first test sequence and the following ones to the convolution with the second overshoot, which is much more pronounced in the first run. The same behavior is present in a 2% solution of the same copolymer (Figure 6a). The most

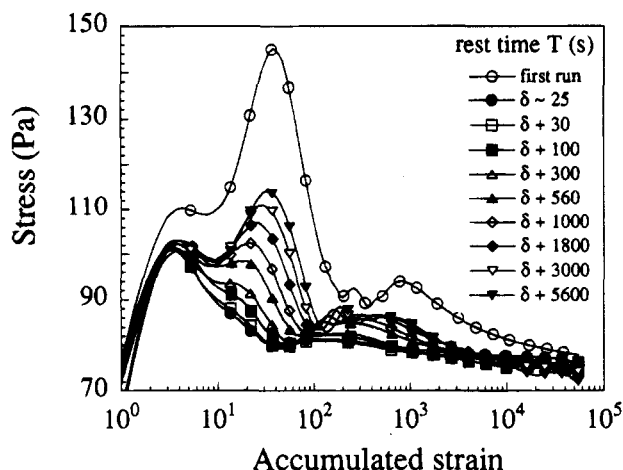


**Figure 5.** Influence of rest time between successive shear rate steps on the transient stress behavior: copolymer F, 3% w/w,  $\dot{\gamma} = 56 \text{ s}^{-1}$ . Only one out of thirty experimental points is pictured as a symbol.  $\delta$  is the time delay,  $\approx 25 \text{ s}$ , needed to store one experiment.

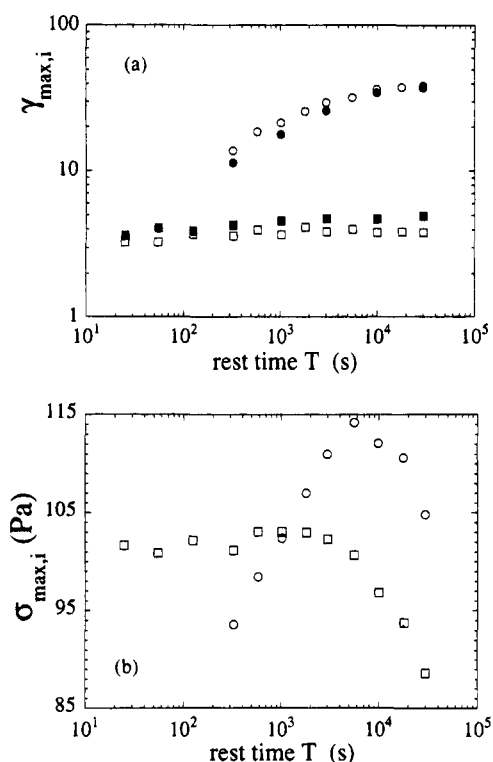


**Figure 6.** Influence of rest time between two successive shear rate steps on the position (a) and amplitude (b) of the first (squares) and second (circles) stress overshoots. Sample is copolymer F: open and closed symbols denote respectively 3 and 2% w/w concentration.

significant overshoots are observed during the first shear rate step. In the immediately following step, the overshoots with an order higher than one nearly vanish and they begin to increase again with increasing rest time. It is worthwhile to note that the overshoot in the corresponding homopolymer solution, which is comparable to the first overshoot in the copolymer solution, is completely insensitive to the rest time  $T$ , at least if  $T > 25 \text{ s}$ , which is the minimum value imposed by data storage between two successive experiments.

Figure 7 shows the relative variations of the height and position for the second overshoot as a function of rest time, their values measured during the first shear step being used as references.

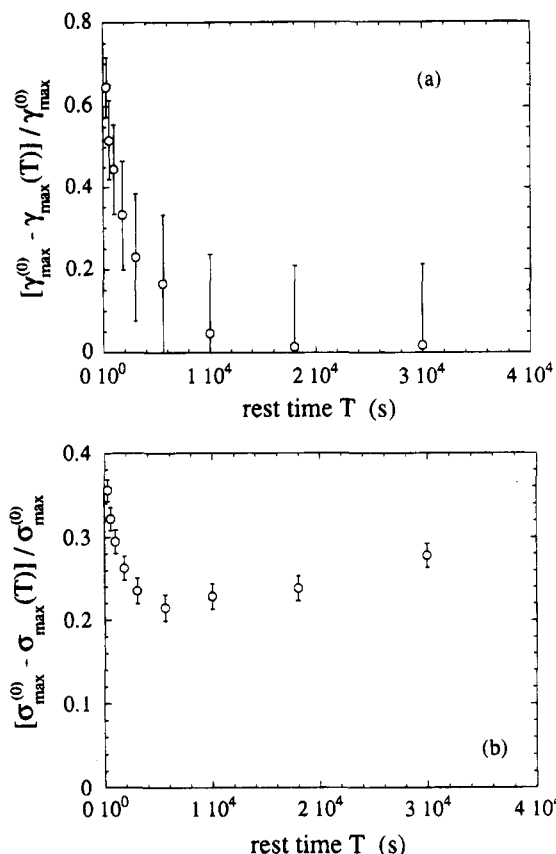


**Figure 7.** Relaxation with rest time of the position (a) and amplitude (b) of the second overshoot to their initial values  $\gamma_{\max}^{(0)}$  and  $\sigma_{\max}^{(0)}$  during the first shear rate step: copolymer F, 3% w/w.

**3.3. Long-Term Evolution.** Aging processes are also an important feature of these associative copolymers: solutions aging at rest in the dark show a decrease of their viscosity-enhancing properties with time. This effect was found to occur faster for samples obtained at full conversion of the copolymerization reaction, i.e., for samples with a larger heterogeneity in chemical composition and a smaller average hydrophobe content. A slight increase in temperature seems to accelerate this phenomenon. Figure 8 shows the time evolution of the viscosity vs shear rate curves for sample A with 85% conversion (Figure 8a) and for sample F with 11.3% conversion (Figure 8b). The corresponding homopolymers of similar molecular weight show a known decrease of viscosity, thoroughly investigated by Kulicke et al.<sup>11</sup> This time-dependent evolution of the polyacrylamide occurs only for molecular weights above  $1.5 \times 10^6$  and is dependent on the molecular weight itself. Kulicke has found a decrease of viscosity of about 20% during 40 days for a polymer of  $\bar{M}_n = 3.3 \times 10^6$ . Thus both the amplitude and the time scale of this phenomenon differ markedly from the ones evident in Figure 8.

## 4. Discussion

**4.1. Stress Relaxation.** As depicted in Figure 3, two different behaviors can be distinguished for the stress relaxation curves according to the magnitude of the shear rate. At low shear rates, a small part of the relaxation process occurs in a short time ( $t \approx 50 \text{ s}$ ), followed by a slow relaxation with a constant characteristic time of about 900 s. For larger shear rates, the major part of the stress relaxes on a short time scale,

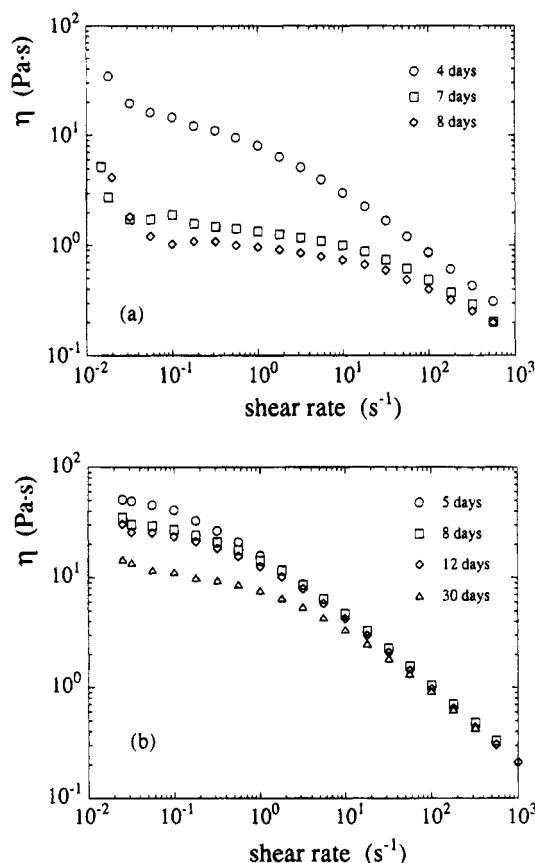


**Figure 8.** Aging effects on the steady-state viscosity vs shear rate curves: (a) copolymer A; (b) copolymer F. See Table 1 for the characteristics of the samples.

and the slow relaxation seems to disappear in the limit of experimental accuracy.

This behavior could be understood qualitatively by ascribing it to the influence of hydrophobic associations. At small shear rates, the hydrophobic domains are not disrupted by the flow, and the stress relaxation is essentially due to the rearrangement of the chains through their partial dissociation and recombination. Then the corresponding long relaxation time would result from the cooperative effects of these processes<sup>12</sup> and should depend on their respective rates through the total hydrophobic monomer content, the distribution of hydrophobic blocks, and the polymer concentration. On the other hand, at high shear rates, disrupted blocks would play only a minor role and the stress relaxation would occur as in homopolymer solutions mainly through a disengagement of the chains, although possibly slightly hindered by the influence of hydrophobic blocks as we shall discuss later on. Then the stress relaxation can no longer be followed with the instrument as in most polymer solutions. If we make the assumption that the borderline between the two behaviors is reached for shear rates comparable to the inverse lifetime  $1/\tau_{\text{life}}$  of the domains, then we get the estimation  $\tau_{\text{life}} \approx 1$  s. However, we shall see in the next section that this simple analysis raises some difficulties.

**4.2. Stress Overshoots.** The presence of stress overshoots upon the establishment of a steady shear flow is well documented for entangled polymer systems.<sup>13,14</sup> The classical explanation for these phenomena links their appearance to strain rates larger than the smaller relaxation rate  $1/\tau_d$  in the system, where  $\tau_d$  is the disengagement time of the chains. As  $\dot{\gamma}\tau_d$  becomes larger than 1, the orientation of chains in the flow can

no longer follow the deformation rate, and a transient stress overshoot appears until a steady-state alignment of the chains is realized. This critical shear rate also corresponds to the appearance of significant shear-thinning effects. These overshoots are located at approximately constant strain values of about 2, in reasonable agreement with the Doi-Edwards model.<sup>14</sup> For still higher shear rates, when  $\dot{\gamma} \approx 1/\tau_{\text{eq}}$ , overshoots in the first normal stress difference appear and when  $\dot{\gamma} > 1/\tau_{\text{eq}}$ , the overshoots in the shear stress occur at strain values that increase linearly with the shear rate. Here  $\tau_{\text{eq}} = \tau_d/3Z$  is proportional to the longitudinal Rouse time of the chains and  $Z$  is the number of entanglements. Thus these phenomena are linked with the stretching of the chains in the flow.<sup>14-16</sup> When that stretching is explicitly taken into account, the location of the shear stress overshoots is predicted to vary as  $\dot{\gamma}\tau_{\text{eq}}/2$ ,<sup>16</sup> in good agreement with experiments.<sup>13</sup> Considering the behavior observed with the homopolymer solutions (continuous line in Figure 4), the above analysis would yield  $\tau_d \approx 1$  s,  $\tau_{\text{eq}} \approx 0.04$  s, and  $Z \approx 8$  for a 3% w/w polyacrylamide solution. This relatively small  $\tau_d$  value is consistent with the fact that the stress relaxation is not easily observable for the polyacrylamide solutions.

The behavior of the copolymer solutions is much more complicated. The position of the first overshoot corresponds roughly, at least for the highest shear rates, with that observed in the homopolymer solution with the same concentration and molecular weight. Moreover, its height and position are independent of the time lag between two successive experiments, and thus it is reasonable to think that, at high shear rates, it reflects the same phenomena as in the homopolymer solution. Its behavior at smaller shear rates is less clear: the apparent slight decrease of its strain position for increasing shear rates and its appearance for larger shear rates than in the homopolymer solution are not understood within the above picture. In particular, for shear rates above  $0.5 \text{ s}^{-1}$ , we expect from the results of the shear stress relaxation that most of the hydrophobic domains are disrupted and that the disengagement time in the copolymer solutions is about the same or slightly larger in the homopolymer solutions. This would imply the appearance of that overshoot as soon as  $\dot{\gamma} \geq 1 \text{ s}^{-1}$ , in contradiction with the experimental behavior. However, it is possible that such effects are masked by the second overshoot that appears sooner with a very strong amplitude compared to the first one. The latter would then correspond to the shoulder that seems to develop for shear rates above  $0.32 \text{ s}^{-1}$  in Figure 1a. A last possibility is that the above picture is too simplistic, and this possibility is examined below.

The overshoots that occur at higher strains are observed only with the copolymer solutions and are definitely linked to the presence of hydrophobic units. Tanaka and Edwards<sup>17-20</sup> have proposed a model for solutions of polymers with associative end groups. They have worked out a detailed description of the rheological behavior of such systems, including their transient behavior upon start up of a steady shear flow.<sup>20</sup> In this model, stress overshoots are linked with a junction breakage rate that depends on the stretching of the elastic chains. The strain position of the stress overshoot is predicted to increase linearly with the shear rate. Clearly, this is not consistent with our experimental findings. However, the model is concerned only with small unentangled chains. Therefore it predicts only one overshoot in contrast with the complicated

transient stress behavior observed in our entangled solutions of copolymers with many associating blocks randomly distributed along the chains.

A model much more appropriate to this situation has been proposed by Leibler, Rubinstein, and Colby.<sup>12</sup> They derived the self-diffusion coefficient of the chains and the time-dependent shear relaxation modulus by using the concept of sticky reptation where the chain reptation is slowed down by the presence of temporary cross-links. Although sticky reptation might well be a relevant mechanism in our systems, their predictions are not directly fitted to our experiments since they deal only with linear viscoelastic properties and they are made by assuming that thermal equilibrium is always satisfied.

This condition is not fulfilled in our systems where strong hysteresis effects are observed. They have already been noticed in measurements of the shear viscosity vs shear rate along thixotropic loops. In such experiments, the initial zero-shear viscosity is recovered sometimes only after several hours of rest. Thus the solutions need a long time to build again all the hydrophobic domains that have been disrupted by the shear flow. The same conclusion arises from the evolution with rest time of the strain position of the second overshoot (Figure 7a). The amplitude of that overshoot shows the same feature although for long rest times the decay to initial amplitude value is not observed, possibly due to some experimental artifacts (Figure 7b). From the time evolution of the strain position, we can estimate a characteristic time of about 5000 s for the initial state of the solution to be recovered.

An intriguing point concerns the critical shear rate and the strain position associated with the appearance of the second overshoot. The critical shear rate is about 10 times smaller than the one associated with the first overshoot. Following the classical picture described above, this would correspond to a hindered reptation time larger by a factor of 10 compared to a homopolymer solution. This picture is rather consistent with the observation of the copolymer overshoot alone in the range  $0.1 < \dot{\gamma} \text{ (s}^{-1}\text{)} < 1$  and with the fact that stress relaxation curves suggest a breaking of the hydrophobic domains for  $\dot{\gamma} > 0.5 \text{ s}^{-1}$ . However, the fact that both the first and the second overshoots can be observed for high enough shear rates ( $\dot{\gamma} > 1 \text{ s}^{-1}$ ) is rather puzzling within this description.

On the other hand, the picture of junction snapping as proposed by Tanaka and Edwards<sup>17-20</sup> could be at first sight rather appealing to explain the constant value for the strain position of the second overshoot: the transient network would be able to withstand a given amount of strain before a significant amount of elastically active junctions breaks. Assuming that the accumulated strain is the criterion that determines the junction snapping means that, as the shear rates increases, the transient network is able to withstand increasing transient stress levels before its breakage as in entangled polymer systems. However, this picture is not consistent with the appearance of the first overshoot at smaller strains for high enough shear rates. This would mean that the copolymer chains are able to disentangle with a characteristic time close to that in the homopolymer solutions before the transient associative network is broken.

Thus neither of the two pictures, sticky reptation or junction snapping, is fully consistent with the experimental behavior. It seems that this failure is linked to

the implicit assumption made in both models that the associative transient network is well connected. A better understanding of the experiments seems to be possible if the assumption of a loose associative transient network is made. This is in close analogy with the model of heterogeneous cross-linking density proposed to describe the structure of irreversible gels obtained by random cross-linking of entangled chains.<sup>21</sup> The solution might be viewed as an assembly of temporarily connected clusters that are not necessarily well above their gel point. In fact, for such systems, thickening properties can be obtained even below the gel point of the clusters. The second overshoot would then arise from a contribution of the clusters, whether it should be associated with their characteristic size or with their whole size distribution being not clear as yet. The first overshoot would then be observable because a fraction of free chains not included in the clusters is always present until the gelation reaction is complete.<sup>22</sup> For reversible cross-links that condition is never met. The shear flow probably breaks partly the clusters, thus modifying their size distribution and decreasing the shear viscosity in a thixotropic loop. The hysteresis effects observed in the latter experiment as well as those seen with the second overshoot behavior would then reveal the long time needed to restore the initial size distribution of clusters through a slow gelation process. In that picture, the stress relaxation upon cessation of flow can no longer be connected with a single sticky reptation time but probably reflects complicated averages involving the relaxation of free chains and of clusters with a size distribution depending on the shear rate.

**4.3. Long-Term Evolution.** The time evolution of the solutions involves time scales still much longer than hours as shown in Figure 8. A decay of the thickening properties of the copolymers occurs upon ageing of the solutions on time scales of weeks. As reported above, this effect is faster for samples synthesized at full conversion. A possible explanation for that feature can be formulated based on the larger chemical heterogeneity of the chains in these samples. Chains synthesized at the beginning of the copolymerization have a larger than average content of hydrophobic units and hydrophobic block length while chains formed at the end of the reaction are nearly pure polyacrylamide. Both types of chains are intimately mixed upon the washing and precipitation in organic solvents. However, once dissolved again in water, it seems likely that the formation of hydrophobic domains could be associated with a tendency to progressive phase separation of the two types of chains, with the entropic penalty compensated by the decreasing surface to volume ratio of the growing hydrophobic domains. This separation could occur on relatively short time scales because many chains are nearly pure homopolymers and thus move with a basically unaltered reptation mechanism. On the other hand, in solutions of copolymer chains with similar composition, the driving force to separation would be smaller since more chains would have to be constrained in order to grow domains and moreover a larger fraction of them move much more slowly by the sticky reptation mechanism. Thus one could expect a much larger stability of their rheological properties. It would be interesting to investigate the structure of ageing solutions by means of small-angle scattering techniques and test the validity of this hypothesis.

## 5. Conclusions

The transient behavior of solutions of copolymers with randomly distributed associating blocks shows the existence of a number of relaxation processes with characteristic times spanning a very broad range up to  $10^4$  s. As a consequence, sheared solutions are most of the time out of equilibrium systems, and that feature has to be taken into account to investigate their rheological properties.

On an even longer time scale ( $\approx 10^6$  s), ageing of the solutions takes place, and this is tentatively attributed to a trend to phase separation with kinetics depending on the heterogeneity in the chemical composition of the chains.

Upon start up of a steady shear flow, several stress overshoots can be observed depending on the shear rate. The first of them can be identified with the one observed in homopolymer solutions and is independent of shear history. The other ones are linked to the presence of hydrophobic units, and their strain position and amplitude depend on the shear history. If enough rest time is allowed between two successive experiments, the strain position of these overshoots is a constant and does not depend on the shear rate. The critical shear rates and the strain position that characterize the appearance of the overshoots are difficult to understand if the associative transient network is supposed to be well connected. On the other hand, the hypothesis of a loose associating transient network seems to facilitate the interpretation of the overshoot behavior.

Within this hypothesis, stress relaxation curves would reflect complex relaxation mechanisms involving free chains and temporary clusters with a size distribution depending on shear rate.

At present, we consider that picture only as a guide for future work.

Following the suggestions made by a referee, a few remarks can be added. Considering the complex structure of these solutions inferred from our experiments, it could be even doubtful that a zero-shear viscosity can be easily defined in these systems since the attainment of a true equilibrium condition is probably difficult by simply dissolving the polymers. In fact, the preparation of the samples always involves a stirring step and a rest time, which were found necessary to obtain reproducible measurements.<sup>6,7</sup> The proportion of the inter- and intrachain linkages might well change upon stirring or shearing but the present experiments do not provide any information about that point, which should be checked by experiments designed for this aim.

**Acknowledgment.** We are deeply grateful to S. J. Candau for having initiated this work, for his continuous interest, and for many stimulating and helpful discussions. We also warmly thank J. Selb for advice and kind help during the synthesis of the samples and for a careful reading of the manuscript. This work has been supported by a PIRMAT joint program.

## Note Added in Revision

When this paper was completed, we became aware of two recent works somewhat related to the ideas developed here. In the first one by Groot and Agterof,<sup>23</sup> numerical simulations of associative polymer solutions were performed where gelation phenomena and size distribution of associating clusters were explicitly considered. The phase diagram of these systems and their rheological behavior were investigated. Direct comparison with our experiments is however difficult due to the many simplifying assumptions used to facilitate the simulation. An even more recent work by Annable and Ettelaie<sup>24</sup> investigated phase separation in mixtures of associative polymers with hydrophobic end groups and the corresponding unmodified homologues. The occurrence of phase separation was observed to depend on the mixture composition. Interestingly, the two phases were found to have the same overall polymer concentration but different compositions, in very good agreement with the model developed by the same authors.<sup>24</sup>

## References and Notes

- (1) Landoll, L. J. *J. Polym. Sci., Polym. Chem. Ed.* **1982**, *20*, 443.
- (2) Evani, G. D.; Rose, S. *Polym. Mater. Sci. Eng.* **1987**, *57*, 477.
- (3) Glass, J. E. *Polymers in Aqueous Media: Performance through Association*; Advances in Chemistry 223; American Chemical Society: Washington, DC, 1989.
- (4) McCormick, C. L.; Bock, J.; Schulz, D. N. *Encyclopedia of Polymer Science and Engineering*, 2nd ed.; Wiley-Interscience: New York, 1989; Vol. 17.
- (5) Valint, P. L., Jr.; Bock, J.; Schulz, D. N. *Polym. Mater. Sci. Eng.* **1987**, *57*, 482.
- (6) Hill, A.; Candau, F.; Selb, J. *Macromolecules* **1993**, *26*, 4521.
- (7) Biggs, S.; Hill, A.; Selb, J.; Candau, F. *J. Phys. Chem.* **1992**, *96*, 1505.
- (8) Lacfk, I.; Selb, J.; Candau, F. *Polymer*, accepted for publication.
- (9) Fonnum, G.; Bakke, J.; Hansen, F. K. *Colloid Polym. Sci.* **1993**, *271*, 380.
- (10) Annable, T.; Buscall, R.; Ettelaie, R.; Wittlstone, D. *J. Rheol.* **1993**, *37*(4), 695.
- (11) Kulicke, W.-M.; Klein, J. *Angew. Makromol. Chem.* **1977**, *69*, 189.
- (12) Leibler, L.; Rubinstein, M.; Colby, R. H. *Macromolecules* **1991**, *24*, 4701.
- (13) Menezes, E. V.; Graessley, W. W. *J. Polym. Sci., Polym. Phys. Ed.* **1982**, *20*, 1817.
- (14) Doi, M.; Edwards, S. F. *The Theory of Polymer Dynamics*; Oxford University Press: Oxford, 1987.
- (15) Pearson, D. S.; Kiss, A. D.; Fetters, L. J.; Doi, M. *J. Rheol.* **1989**, *33*, 517.
- (16) Pearson, D. S.; Herbolzheimer, E.; Grizutti, N.; Marrucci, G. *J. Polym. Sci. Part B: Polym. Phys.* **1991**, *B29*, 1589.
- (17) Tanaka, F.; Edwards, S. F. *Macromolecules* **1992**, *25*, 1516.
- (18) Tanaka, F.; Edwards, S. F. *J. Non-Newtonian Fluid Mech.* **1992**, *43*, 247.
- (19) Tanaka, F.; Edwards, S. F. *J. Non-Newtonian Mech.* **1992**, *43*, 273.
- (20) Tanaka, F.; Edwards, S. F. *J. Non-Newtonian Fluid Mech.* **1992**, *43*, 289.
- (21) Bastide, J.; Leibler, L. *Macromolecules* **1988**, *21*, 2647.
- (22) Stockmayer, W. H. *J. Chem. Phys.* **1944**, *12*, 125.
- (23) Groot, R. D.; Agterof, G. M. *J. Chem. Phys.* **1994**, *100*, 1649.
- (24) Annable, T.; Ettelaie, R. *Macromolecules* **1994**, *27*, 5616.

MA9500953